Instability and Static Liquefaction on Proportional Strain Paths for Sand at Low Stresses

Article *in* Journal of Engineering Mechanics · November 2004

DOI: 10.1061/(ASCE)0733-9399(2004)130:11(1365)

3 authors, including:

Laurent Lancelot
Université des Sciences et Technologies de Lille 1
22 PUBLICATIONS **168** CITATIONS
SEE PROFILE

Isam Shahrour
Université des Sciences et Technologies de Lille 1
279 PUBLICATIONS **1,600** CITATIONS
SEE PROFILE

Instability and Static Liquefaction on Proportional Strain Paths for Sand at Low Stresses

Laurent Lancelot[1]; Isam Shahrour[2]; and Marwan Al Mahmoud[3]

Abstract: The behavior of Hostun RF sand on proportional strain paths at low confining pressures (20 to 100 kPa) is considered in this paper. In such paths, a constant dilation rate is imposed during shear. The usual features of pore pressure increase (contracting material) or decrease (dilating material) are here observed depending upon whether the imposed dilation rate is respectively greater or smaller than the "natural" dilation rate at failure (as measured in a drained test). Particular attention is given to the static liquefaction phenomenon, which is seen to occur for loose as well as dense sand provided the imposed dilation rate is large enough to lead to a continuous pore pressure increase during shear. Instability tests performed at low confining pressures on proportional strain paths show that the instability line is strain path dependent. It does not coincide with the peak deviator stress line in proportional strain paths tests, in general, but does coincide with the line $d^2W=0$ (nil second increment of total work).

DOI: 10.1061/(ASCE)0733-9399(2004)130:11(1365)

CE Database subject headings: Constitutive relations; Laboratory tests; Triaxial tests; Sand; Strain rate; Liquefaction.

Introduction

This paper, as part of an experimental study on Hostun RF sand at low stresses (Al Mahmoud 1997), focuses on proportional strain path tests carried out on isotropically consolidated loose and dense sands.

Stress–strain data from these tests bring data against which constitutive models can be checked, since these models are generally validated using drained triaxial compression or extension tests. Several workshops on the validation of constitutive laws (Gudehus et al. 1984; Saada and Bianchini 1988) have shown the necessity to check these laws on more complex paths, specifically close to those really induced in situ by structures, such as foundations and tunnels. Besides, the study of shallow structures or soil masses likely to undergo static or cyclic loading leading to low effective stresses requires that experiments be made in the low stress range. Special attention is given to proportional strain dilating tests, where interstitial fluid is forced inside the sample, resulting in a pore pressure increase. They form the basis of the study of static liquefaction and instability phenomenon in the low stress domain presented in the present paper. The analysis of landslides in fine sand or silt deposits has emphasized the practical importance of this phenomenon (see, e.g., Castro and Poulos 1977; Kramer and Seed 1988; Lade 1992; Di Prisco et al. 1995; Konrad and Watts 1995).

In mechanical terms, stability is obtained if a small load increment yields a small strain increment. The theoretical basis for the concept of stability is Drucker's postulate (Drucker 1959). Instability for soils has been investigated through experimental results. Sladen et al. (1985) found that for loose sand in undrained triaxial tests at different initial confining pressures the points of peak deviator stress q in a q–p' plane are on a same line. The position of this line varies with the initial density of sand, hence defining a *collapse surface* in a p'–q–void ratio space. Lade (1992) using theoretical and experimentally based arguments identified an *instability line*, above which instability may occur under certain conditions, and which can be approximated by the line joining the points of peak deviator stress. These phenomena on undrained paths can be extended to more general proportional strain paths, but are then strain path dependent (Chu et al. 1993).

Based on this theoretical framework, our results of static liquefaction and instability tests are presented and a discussion of these matters in the low stress domain is proposed.

Instability Concept in Literature

Drucker (1959) postulated that stability is assured if the second increment of plastic work is positive, that is

$$d^2W^p = d\sigma_{ij}d\varepsilon_{ij}^p > 0 \tag{1}$$

Hill (1958) extended Drucker's postulate to the second increment of total work.

This postulate is adequate for materials exhibiting associated flow, but may be violated for soils (Lade 1992). Lade's instability conditions are summarized by the following relations:

[1]Assistant Professor, Laboratoire de Mecanique de Lille (CNRS UMR8107), Avenue Paul Langevin, 59655 Villeneuve d'Ascq Cedex, France.

[2]Professor, Laboratoire de Mecanique de Lille (CNRS UMR8107), Avenue Paul Langevin, 59655 Villeneuve d'Ascq Cedex, France.

[3]Research Fellow, Laboratoire de Mecanique de Lille (CNRS UMR8107), Avenue Paul Langevin, 59655 Villeneuve d'Ascq Cedex, France.

Note. Associate Editor: Jin Y. Ooi. Discussion open until April 1, 2005. Separate discussions must be submitted for individual papers. To extend the closing date by one month, a written request must be filed with the ASCE Managing Editor. The manuscript for this technical note was submitted for review and possible publication on February 25, 2003; approved on May 12, 2004. This technical note is part of the ***Journal of Engineering Mechanics***, Vol. 130, No. 11, November 1, 2004. ©ASCE, ISSN 0733-9399/2004/11-1365–1372/$18.00.

$$\begin{cases} d\sigma'_{ij} \cdot d\varepsilon_{ij} < 0 \\ \dfrac{\partial f}{\partial \sigma_{ij}} \delta_{ij} < 0 \\ \dfrac{\partial g}{\partial \sigma_{ij}} \delta_{ij} > 0 \end{cases} \tag{2}$$

where f=loading function; g=plastic potential; and δ=Kronecker tensor. These conditions, in addition to Hill's postulate, stipulate that the normal to the loading surface should be directed toward negative p' (which means that a certain stress level has to be reached) and that volumetric plastic strain should be positive (contraction) for instability to occur.

Chu et al. (1993) used proportional strain path instability tests to show that the occurrence of instability is governed by two parameters: The loading ratio $\alpha=\sigma'_1/\sigma'_3$ and the imposed dilation rate ζ_i. They found that α must be high enough and ζ_i smaller than ζ_f (volumetric strain rate at failure, as measured in drained tests) for instability to occur in instability tests. For the particular case of undrained tests ($\zeta_i=0$), their instability conditions are equivalent to those of Lade. However, the position of the "instability line" is not an intrinsic property of sands: It is found to depend on ζ_i. More recently, Di Prisco et al. (1995) showed that this "instability line" for undrained paths is also a function of initial consolidation—isotropic or anisotropic—and preloading (e.g., overconsolidation).

Experimental Setup and Procedure

Test Setup

In the determination of mechanical properties of sands at low stresses, technical problems arise mainly in sample preparation, stress and strain measurement, and testing method.

Friction between the sample and platens has to be carefully controlled in element tests, because it can dramatically reduce sample homogeneity, causing sample bulging or strain localization in shear bands. Most authors agree that samples should be in a 1/1 height-to-diameter ratio (e.g., Lee 1978), with properly lubricated platens, covered with rubber sheets that can deform radially, hence reducing end retraint to a minimum. The system used in this study is detailed in Al Mahmoud (1997).

The triaxial cell is equipped with a waterproof force transducer (0–2500 N, 0.5% nonlinearity) placed inside the cell underneath the base platen. Axial strain is measured by a linear strain conversion transducer placed outside the cell (range 25 mm, 0.1% nonlinearity). Cell pressure (resp. back pressure) is controlled by a digital pressure–volume controller (Menzies 1988) within a 0–2 MPa range (resp. 0–400 kPa) with 1 kPa resolution (resp. 0.1 kPa). Sample volume change can be measured with a 1 mm^3 resolution using the back pressure controller.

In low stress triaxial compression tests, membrane rigidity has to be considered when the sample deforms, even if thin membranes (0.2 mm) are used, since an extra radial stress is added to the effective confining pressure. This extra stress was computed as shown in Fukushima and Tatsuoka (1984) and, as an example, it was found that an overestimation of ϕ' of about 1° can occur if the influence of the membrane is neglected in a drained triaxial compression test with a 20 kPa confining pressure (Al Mahmoud 1997).

At low stresses, other factors must be considered (Fukushima and Tatsuoka 1984; Tatsuoka et al. 1986; Kolymbas and Wu 1990): Bedding error, sample self-weight, and top platen weight. Bedding error, which can be a major concern when elastic modulus has to be measured, was disregarded. Sample self-weight and top platen weight were estimated to account, respectively, for an extra deviator stress of 0.3 and 0.6 kPa in our case.

Experimental Procedure

The sand used was Hostun RF sand, a subangular medium sand (D_{50}=0.471 mm, C_u=2.26, γ_s=25.96 kN/m^3, e_{min}=0.575, and e_{max}=0.943). Samples were prepared by pouring a known mass of air dry sand in the mold, by deposition with a spoon for loose samples, but in five lifts for dense samples, each was tamped using a steel rammer.

Saturation was achieved through the carbon dioxide method (Lade and Duncan 1973). Tests have been performed with back pressures ranging from 250 to 300 kPa, on samples with Skempton's B parameter greater than 0.96. The cell pressure controller volume change reading during saturation gave an estimate of sample volume change during this stage. The back pressure controller volume change reading during consolidation was then used to compute the initial sample void ratio before testing.

Proportional Strain Path Tests

Principle and Testing Procedure

Triaxial proportional strain path tests are performed by imposing a constant radial to axial strain ratio, which means that a constant rate of volumetric strain $\zeta=\Delta\varepsilon_v/\Delta\varepsilon_1$ is imposed. Oedometric tests and triaxial undrained tests are thus special cases with an imposed ζ (noted ζ_i hereafter) of 1 and 0, respectively.

After the saturation and consolidation stage is completed, the contact between ram and sample must be established very carefully since any axial strain change results in an imposed proportional volume change, since samples are sheared at a constant axial strain rate, with an imposed volumetric strain increment $\Delta\varepsilon_v$ such that $\zeta=\Delta\varepsilon_v/\Delta\varepsilon_1$ is constant.

Triaxial proportional strain path tests have been performed on loose and dense sand for 20 and 50 kPa initial confining pressures and several values of ζ_i (see Table 1).

Contractive Proportional Strain Paths ($\zeta_i>\zeta_f$)

Results for tests DP4 to DP6 and CIU1 for initial confining pressure σ'_0=20 kPa on loose sand are presented in Figs. 1(a and b). ζ_i for these tests range from 0 to 1. A drained test on loose Hostun RF sand for σ'_0=20 kPa yielded a volumetric strain rate at failure $\zeta_f=-\tan\psi_{max}=-0.075$ (Al Mahmoud 1997).

The pore pressure decrease, due to pore fluid forced out of the sample, results in an effective confining pressure increase, especially if ζ_i is larger [Fig. 1(a)]. The p'–q plot [Fig. 1(b)] shows that past an initial decrease in p', the effective mean pressure increases and an almost linear p'–q curve is obtained, indicating a rapid stabilization of the q/p' ratio for this kind of strain path, and the fact that this ratio decreases when ζ_i increases (because the imposed strain path then gets closer to isotropic).

Results of tests for a 20 kPa initial confining pressure on dense sand ($\zeta_f=-0.92$) are presented in Fig. 2. A very dilative behavior is globally observed, with a pore pressure decrease resulting in an increase of the lateral stress [Fig. 2(a)]. Lateral stress swiftly reaches high stresses with a higher rate than that observed on

Table 1. Initial Properties of Samples Tested in this Study

Test	Test type	Consolidation pressure (kPa)	Initial void ratio $e(-)$	Dry specific weight γ_d (kN/m^3)	Density index $I_D(-)$	Imposed volumetric strain rate $\zeta_i(-)$
CIU1	Undrained triaxial compression	20	0.913	13.57	0.082	0
CIU2		50	0.920	13.52	0.064	0
CIU3		20	0.610	16.13	0.905	0
CIU4		50	0.610	16.13	0.905	0
DP1	Proportional strain path (imposed dilation rate)	20	0.908	13.61	0.096	−0.50
DP2		20	0.908	13.61	0.096	−0.20
DP3		20	0.908	13.61	0.096	−0.10
DP4		20	0.894	13.71	0.133	0.20
DP5		20	0.894	13.71	0.133	0.50
DP6		20	0.894	13.71	0.133	1.00
DP7		20	0.606	16.16	0.915	−1.40
DP8		20	0.606	16.16	0.915	−1.20
DP9		20	0.610	16.13	0.905	0.50
DP10		20	0.606	16.16	0.915	1.00
DP11		50	0.920	13.52	0.064	−0.50
DP12		50	0.920	13.52	0.064	−0.20
DP13		50	0.920	13.52	0.064	−0.10
DP14		50	0.920	13.52	0.064	0.20
DP15		50	0.920	13.52	0.064	0.50
DP16		50	0.920	13.52	0.064	1.00

loose sand [Fig. 1(a)]. The evolution of deviator stress is similar to that observed in loose sand [Fig. 2(b)]: Rapid increase of q with p', then almost linear evolution, the rate of change of q with p' being smaller when ζ_i is larger.

Dilative Proportional Strain Paths ($\zeta_i < \zeta_{max}$): *Static Liquefaction*

General Behavior

Results on loose sand for a 20 kPa initial confining pressure are presented in Figs. 1(c and d). Tests DP1 to DP3 correspond to values of ζ_i ranging from −0.5 to −0.1 (with $\zeta_f = -0.075$ in this case). The effective radial stress decreases down to zero during shearing [Fig. 1(c)]. As a consequence, a static liquefaction is obtained. Liquefaction is due to the pore pressure increase induced by the pore fluid flow forced into the sample: The greater the imposed dilation rate, the faster the radial stress decreases to zero [Fig. 1(c)]. The slightly negative final values of lateral effective stress σ'_3 for $\zeta_i = -0.5$ may be attributed to a lack of precision in the imposed path for highly dilative proportional strain paths. The peak deviator stress [Fig. 1(d)] corresponds to a mobilized friction angle of about 15°, much smaller than the friction angle at failure for drained tests (38.3°). Fig. 1 also shows that peak resistance is lower when the imposed dilation rate is higher (ζ_i more strongly negative).

For $\zeta_i = -0.1$ close to ζ_f (test DP3), the effective radial stress decrease is slower than that for $\zeta_i < \zeta_f$ and does not cancel at the end of the test. The deviator stress [Fig. 1(b)] shows two relative maxima. The first stress peak occurs inside the failure surface, whereas the second deviator peak lies on the failure surface.

For dense sand and $\zeta_i = -1.4$, it is seen that lateral effective stress sharply decreases when axial strain increases at the beginning of test [Fig. 2(c)], then gradually tends to zero. For $\zeta_i = -1.2$, a fast drop to an almost zero value is observed, then the effective lateral pressure slightly increases again and reaches a local maximum for an axial strain of 4% and gradually decreases again to zero. For the deviator stress curve [Fig. 2(d)], the behavior is similar to that observed for loose sand and $\zeta_i = -0.1$: A first peak is reached, corresponding to a mobilized friction angle of 25°, then a second along the failure line (mobilized friction angle 50°, corresponding to the friction angle at failure in this range of stress).

The presence of two stress peaks may be explained by the variation of the material rate of volumetric strain due to changes in the stress state. This rate is known to increase with mean pressure p', and it tends to zero for large axial strains. At the beginning of the test, ζ_i is less than the material rate of volumetric strain and the material exhibits a peak of deviator stress, then the failure line is reached and, for this state of stress, ζ_i becomes greater than the material rate volumetric strain because this one decreases when p' decreases. The material then exhibits a p' and q increase along the failure line until a maximum value is reached. As the material rate of volumetric strain tends to zero for a certain level of axial strain, ζ_i exceeds it again and both p' and q decrease to zero (static liquefaction).

Static Liquefaction

Soil behavior is governed by the combination of three parameters: Density, confining pressure, and drainage conditions. For a drained triaxial test, deviator stress $q = \sigma'_1 - \sigma'_3$ and effective loading ratio $\alpha = \sigma'_1/\sigma'_3$ reach their maximum simultaneously. Conversely, for an undrained triaxial test on sufficiently loose sands, q is known to quickly increase to its maximum, then decrease to a residual value, whereas α increases monotonously until it reaches its failure value α_{max}. Static liquefaction corresponds to this loss of material resistance under undrained shear, due to a pore pressure increase. It has been shown to be the cause of landslides and flows (e.g., Konrad and Watts 1995). It has been observed in undrained triaxial tests for conventional consolidation stresses

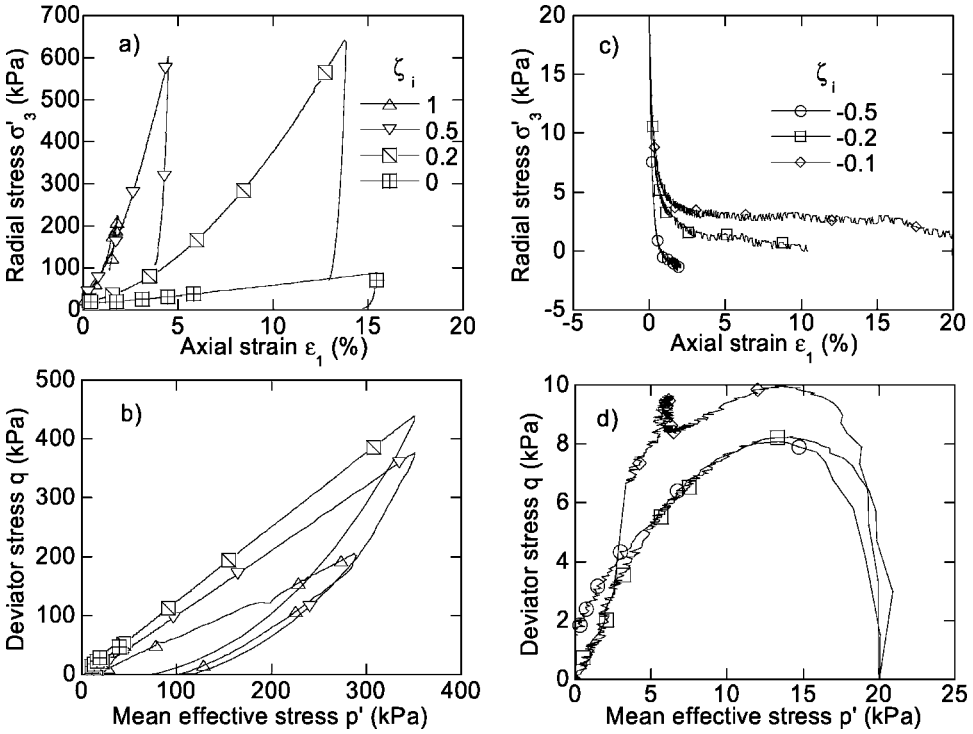

Fig. 1. Proportional strain tests on loose Hostun RF sand for 20 kPa initial confining pressure

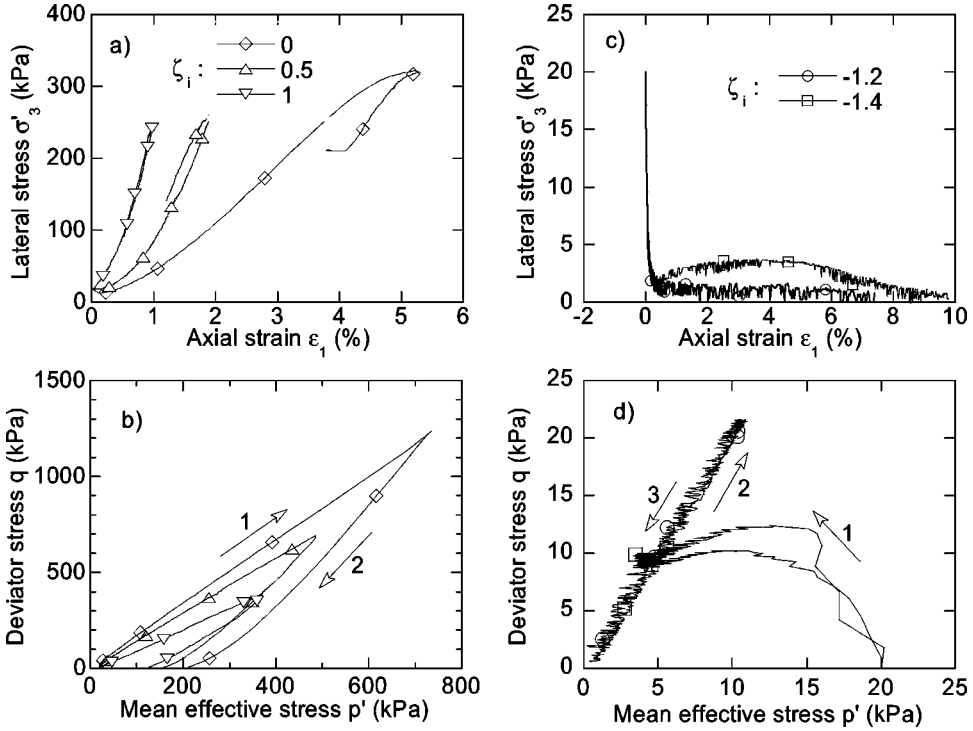

Fig. 2. Proportional strain tests on dense Hostun RF sand for 20 kPa initial confining pressure

Table 2. Results for Instability Tests on Hostun RF Sand

Test	Density index I_D (−)	Confining stress σ'_0 (kPa)	Stress level α (−)	Imposed volumetric strain rate ζ_i (−)	Outcome
IL01	0.07	50	2.97	−0.2	Unstable
IL02	0.08	50	1.98	−0.2	Unstable
IL03	0.06	50	1.89	−0.2	Unstable
IL04	0.07	50	1.76	−0.2	Stable
IL05	0.07	50	1.79	−0.2	Stable
IL06	0.07	20	1.91	−0.2	Unstable
IL07	0.06	20	1.73	−0.2	Stable
ID01	0.92	50	4.41	−1.2	Unstable
ID02	0.92	50	3.68	−1.2	Unstable
ID03	0.91	50	2.62	−1.2	Unstable
ID04	0.91	50	2.48	−1.2	Unstable
ID05	0.93	50	2.34	−1.2	Stable
ID06	0.92	20	2.95	−1.2	Unstable
ID07	0.93	20	2.79	−1.2	Unstable

(Castro 1969; Sladen et al. 1985; Konrad 1990), and in more general proportional strain path tests (Chu et al. 1993).

As illustrated in Fig. 2(b), undrained tests on loose sand at low confining pressures exhibit a steady rise in deviator stress, after a local stabilization corresponding to the phase transition between contracting and dilating behavior. This behavior is generally observed in undrained tests on medium dense or dense sands under conventional consolidation stresses. It indicates that for low confining pressures, the excess pore pressure generated during undrained shear of loose samples is insufficient to produce static liquefaction. Drained tests for the same confining pressures and initial density show a dilative behavior of Hostun RF sand, and isotropic compression tests show that samples are overconsolidated for confining pressures less than 340 kPa (Al Mahmoud 1997; Lancelot et al. 2003). Very loose samples (negative I_D) can be prepared by the moist-tamping method described, for instance, by Konrad (1990). This writer has obtained static liquefaction for such samples, though at confining pressure exceeding 100 kPa. Canou et al. (1991) and Doanh et al. (1997) obtained static liquefaction of very loose Hostun RF sand samples for confining pressures as low as 50 kPa.

However, as already shown by Chu et al. (1992), and as illustrated in Fig. 2(d), dense sand can undergo static liquefaction provided $\zeta_i < \zeta_f$. Given the low values of initial confining pressure used in the present study, which result in a very dilative behavior for dense sand, the value of ζ_i required to trigger static liquefaction is strongly negative, and test control on such paths is more difficult.

Instability of Sand at Low Stresses

For such loading paths where static liquefaction can occur, if triaxial loading is stress controlled, the sample may fail to sustain a given state of stress after the maximum deviator stress has been reached (e.g., Castro 1969). Lade et al. (1987, 1988) showed that samples loaded to a state of stress located above the peak deviator stress line could exhibit an unstable behavior: If a constant deviator stress is forced on the sample and the drainage valve is closed, then a sufficiently loose sample soon fails.

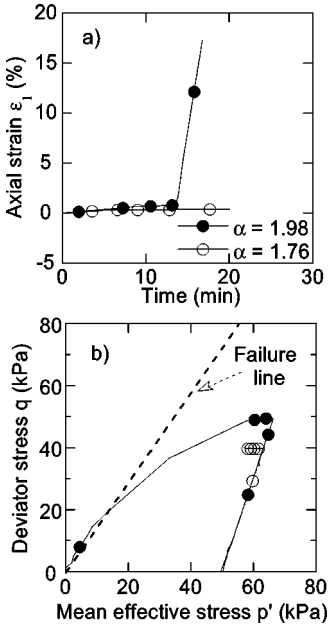

Fig. 3. Typical response of loose Hostun RF sand in stress controlled tests (for $\zeta_i = -0.2$): influence of the loading level α (stability for $\alpha = 1.76$, instability for $\alpha = 1.98$)

In this section, an experimental survey of instability of Hostun RF sand at low stresses is presented. A unified presentation of results for static liquefaction and instability for low stresses is then proposed according to the theoretical framework summarized in the section entitled, "Instability Concept in Literature."

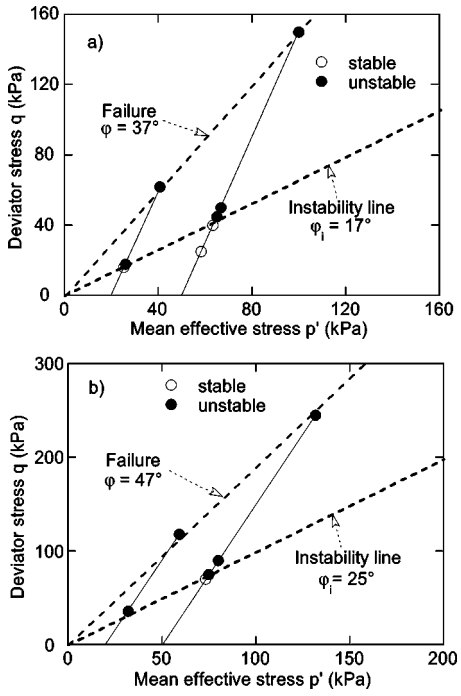

Fig. 4. Instability line between stable and unstable behavior for Hostun RF sand: (a) loose with $\zeta_i = -0.2$ and (b) dense with $\zeta_i = -1.2$

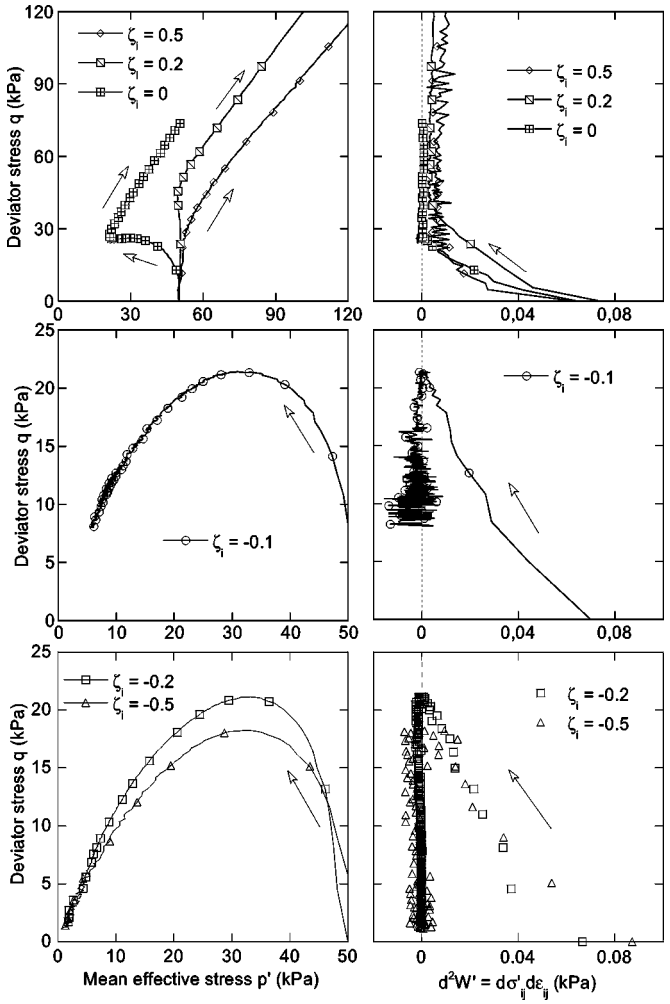

Fig. 5. Stress path and evolution of the second increment of total work (d^2W') on proportional strain tests $\zeta_i > \zeta_f$ (top), $\zeta_i \approx \zeta_f$ (middle) and $\zeta_i < \zeta_f$ (bottom)

Instability Tests

Procedure

The study of instability of sand requires a sophisticated triaxial equipment (Chu et al. 1993; Al Mahmoud 1997). A hydraulically controlled triaxial cell (Menzies 1988) has been used, in which cell pressure, back pressure, and axial stress can be controlled independently. A back pressure of 500 to 600 kPa was used to enhance saturation. Loading is carried out in two steps:

- A given load ratio $\alpha = \sigma'_1/\sigma'_3$ is first imposed by following a drained, strain-controlled path.
- At this stage, the state of total stress (cell pressure and axial stress) is kept constant (stress-control) while the drainage conditions are changed: A constant rate of volumetric strain ζ_i is imposed, so that any small axial strain increment (creep) acting on the sample causes a proportional change in sample volume. If ζ_i is such that the volume change causes a pore pressure increase, then the resulting material loss of resistance may lead to collapse.

Results

Several tests were performed, where values of α_0 were varied up to α_{max} (α peak value), for initial confining pressures of 20 and 50 kPa for loose and dense Hostun RF sand, as listed in Table 2.

As illustrated in Fig. 3, where tests are presented for $\zeta_i = -0.2$ and $\alpha = 1.76$ or $\alpha = 1.98$ (tests IL04 and IL02, respectively), depending on the values of α and ζ_i the state of the sample may either stabilize or run out of control while the sample collapses (instability).

Fig. 4 shows the limit between stable and unstable states as indicated by instability tests listed in Table 2. It is found that the threshold value of α necessary to trigger an unstable behavior is reasonably constant in the range of confining pressure investigated in this study: The limit between stable and unstable states can be considered as a straight line passing through the origin of stress axes. However, the position of this line depends on density. In the Mohr plane, this line defines a friction angle ϕ_i which was found to be around 17° for loose sand and $\zeta_i = -0.2$ and 25° for dense sand and $\zeta_i = -1.2$.

Instability and Static Liquefaction in Proportional Strain Paths

The above results concerning the "domain of instability" for particular values of ζ_i and the initial density will now be compared to the proportional strain path tests leading to static liquefaction, presented in the section entitled, "Proportional Strain Path Tests". It can be seen in instability conditions derived by Lade [Eq. (2)] or Chu et al. that a necessary condition for instability is that the second increment of total work changes sign at the onset of unstable behavior. Hence $d^2W' = d\sigma'_{ij} d\varepsilon_{ij}$ has been computed for proportional strain path tests carried out in this study. The evolution of d^2W' for loose sand is shown in Fig. 5 for ζ_i ranging between −0.5 and 0.5 and $\sigma'_0 = 50$ kPa (for which $\zeta_f = -0.065$). For $0 \leq \zeta_i \leq 0.5$ ($\zeta_i > \zeta_f$), d^2W' decreases to a (positive) minimum, corresponding to a minimum effective mean pressure p', then either stabilizes ($\zeta_i = 0$) or increases as both p' and q increase ($\zeta_i > 0$). Neither static liquefaction nor instability can be observed on such paths, which is in perfect agreement with the fact that d^2W' remains positive. For $\zeta_i < \zeta_f$, a zero second increment of total work is obtained for a deviator stress close to the maximum, then d^2W' remains zero—or marginally negative—until the end of the test. Static liquefaction is obtained for these tests. From Fig. 5, a certain scatter can be observed in the measured values of d^2W', especially for $\zeta_i = -0.1$ (ζ_i smaller than, but close to, ζ_f) and small values of deviator stress q. It should be noted that tests are strain controlled with an imposed $d\varepsilon_1$ in the range of 0.01–0.015%, resulting in $d\sigma'_3$ values in the range of the digital pressure controller resolution.

Fig. 6 shows that the points where d^2W' cancels out in proportional strain path tests for loose Hostun RF sand lie on a straight line passing through the origin, the inclination of which increases when ζ_i decreases. This clearly shows that the instability domain depends on ζ_i. Lines joining peak deviator stresses have a smaller slope. Darve et al. (1995), using numerical simulations, showed that d^2W' along proportional strain paths changes sign before maximum deviator stress is reached if $\zeta_i > 0$, at maximum if $\zeta_i = 0$ and after the maximum if $\zeta_i < 0$. The slope of the line joining maximum deviator stresses also depends on ζ_i: If ζ_i is smaller (or the dilating rate is greater), then the mobilized friction angle at deviator stress peak is smaller.

In Fig. 7, the results of instability tests are superimposed to those of static liquefaction for loose sand and $\zeta_i = -0.2$. It is shown that the $d^2W' = 0$ line lies within the zone $1.79 \leq \sigma'_1/\sigma'_3 \leq 1.91$ which was shown to contain the instability line for these loading conditions (ϕ_i mean value 17.3°). Moreover, the peak deviator stress line also lies in this zone. Hence, for loose sand

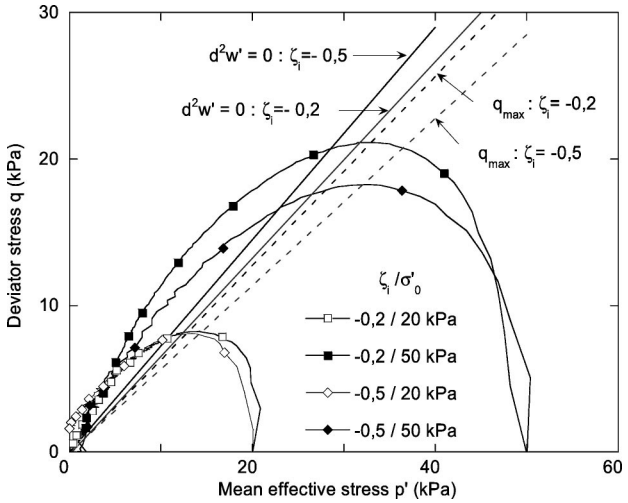

Fig. 6. Comparison between peak deviator stress lines and $d^2W'=0$ lines for loose sand

(where ζ_f is close to zero) and for practical purposes, the line that joins the values of peak deviator stress, the $d^2W'=0$ line and the instability line can be considered as a single line, the position of which depends on the strain path.

Several authors published results on the instability of Hostun RF sand on undrained paths ($\zeta_i=0$). Doanh et al. (1997) published data for isotropically and anisotropically consolidated, compression and extension undrained tests, on very loose Hostun RF sand. They found an average mobilized friction angle at peak ϕ_i for isotropically consolidated samples of 16.8°. This is consistent with our value $\phi_i=17.3°$, given the different loading path ($\zeta_i=-0.2$) and the slightly overconsolidated nature of the samples used in the present study.

Conclusion

Proportional strain path tests were performed on Hostun RF sand to examine the issue of static liquefaction and instability for this sand in the low stress range.

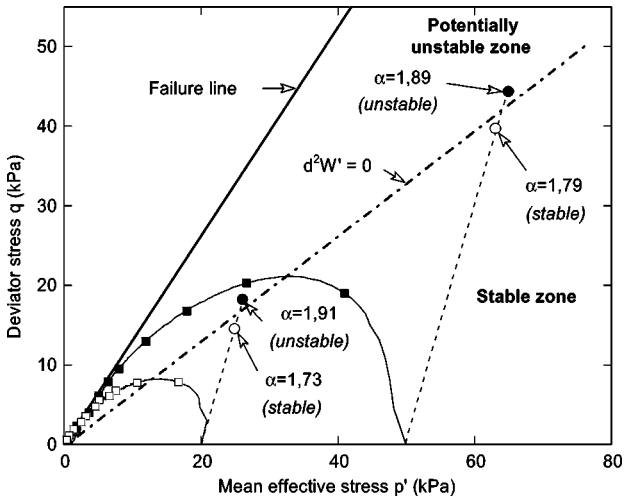

Fig. 7. Instability tests and $d^2W'=0$ line for loose sand and $\zeta_i=-0.2$

It was found that undrained tests (zero-imposed volumetric strain rate ζ_i) on loose sand did not lead to static liquefaction due to sample overconsolidation at low stresses. Proportional strain path tests showed that static liquefaction can be obtained for loose as well as dense sand provided the imposed volumetric strain rate is smaller than the material volumetric strain rate ($\zeta_i<\zeta_f$).

Instability tests performed on loose and dense sand showed that there exists a potential instability zone, delimited by a straight line passing through the origin of stress axes (the instability line) above which a soil element, if submitted to an imposed state of (total) stress and an imposed dilation rate, will collapse spontaneously, under the condition that $\zeta_i<\zeta_f$. However, the position of this instability line depends on the imposed volumetric strain rate. The locus of zero d^2W' was drawn for proportional strain path tests with $\zeta_i<\zeta_{max}$. This was shown to be a straight line passing through the origin of stress axes, the inclination of which is larger when ζ_i is smaller (larger imposed dilation rate). The slope of this line is also larger than the peak deviator stress line, but was found experimentally to be the same as the slope of the instability line. The "instability" or "collapse" line concept is useful for the stability analysis of shallow submerged slopes in an engineering approach (Lade 1992). The simulation of the state of stress in a slope using a properly chosen elastoplastic model is also possible, and was shown by Di Prisco et al. (1995) to better account for the effect of consolidation and preloading of soil in the occurrence of instability. In both approaches, relevant experimental data are needed for the identification and/or validation of the chosen models, and the present study aims at contributing to that purpose.

Notation

The following symbols are used in this paper:

d^2W = $d\sigma_{ij}d\varepsilon_{ij}$; second increment of work;
e = void ratio;
f = loading function;
g = plastic potential;
I_D = density index;
p' = $(\sigma'_1+2\sigma'_3)/3$; mean effective stress;
q = $\sigma'_1-\sigma'_3$; deviator stress;
α = σ'_1/σ'_3; loading ratio;
α_{max} = α value at failure
δ_{ij} = Kronecker tensor;
ε_1 = axial strain;
ε_v = volumetric strain;
ε_{ij} = strain tensor;
ζ = $\Delta\varepsilon_v/\Delta\varepsilon_1$; volumetric strain rate;
σ_{ij} = total stress tensor;
σ'_1 = effective major principal stress;
σ'_3 = effective minor principal stress;
σ'_c = effective consolidation stress;
σ'_0 = effective confining stress;
ϕ = internal angle of friction; and
ϕ_i = mobilized angle of friction at onset of instability.

Subscripts

0 = initial;
i = imposed;
f = failure; and
max = maximum or peak value.

Superscripts

p = plastic.

References

Al Mahmoud, M. (1997). "Etude en laboratoire du comportement des sables sous faibles contraintes." PhD dissertation, Univ. of Lille, Lille, France.

Canou, J., Thorel, L., and De Laure, E. (1991). "Influence d'un déviateur de contrainte initial sur les caractéristiques de liquefaction statique du sable." *Proc., 10th European Conf. Soil Mechanics*, Florence, Italy, ISSMGE, Vol. 1, 49–53.

Castro, G. (1969). "Liquefaction of sand." PhD thesis, Harvard Soil Mechanics Series No. 81, Harvard University, Cambridge, Mass.

Castro, G., and Poulos, S. J. (1977). "Factors affecting liquefaction and cyclic mobility." *J. Geotech. Eng. Div., Am. Soc. Civ. Eng.*, 103(6), 501–506.

Chu, J., Lo, S.-C. R., and Lee, I. K. (1992). "Strain softening behavior of granular soil in strain-path testing." *J. Geotech. Eng.*, 118(2), 191–208.

Chu, J., Lo, S.-C. R., and Lee, I. K. (1993). "Instability of granular soils under strain path testing." *J. Geotech. Eng.*, 119(5), 874–892.

Darve, F., Flavigny, E., and Meghachou, M. (1995). "Constitutive modelling and instabilities of soil behavior." *Comput. Geotech.*, 17, 203–224.

Di Prisco, C., Matiotti, R., and Nova, R. (1995). "Theoretical investigation of the undrained stability of shallow submerged slopes." *Geotechnique*, 45(3), 479–496.

Doanh, T., Ibraim, E., and Matiotti, R. (1997). "Undrained instability of very loose Hostun sand in triaxial compression and extension. I: Experimental observations." *J. Cohesive-Frictional Mater.*, 2, 47–70.

Drucker, D. C. (1959). "A definition of stable inelastic material." *J. Appl. Mech.*, 26, 101–106.

Fukushima, S., and Tatsuoka, F. (1984) "Strength and deformation characteristics of saturated sand at extremely low pressures." *Soils Found.*, 24(4), 30–48.

Gudehus, G., Darve, F., and Vardoulakis, I. (1984). *Constitutive relations for soils*, Balkema, Rotterdam.

Hill, R. (1958). "A general theory of uniqueness and stability in elastoplastic solids." *J. Mech. Phys. Solids*, 6, 236–249.

Kolymbas, D., and Wu, W. (1990). "Recent results of triaxial tests with granular materials." *Powder Technol.*, 60, 99–119.

Konrad, J. M. (1990). "Minimum undrained strength of two sands." *J. Geotech. Eng.*, 116(6), 932–947.

Konrad, J. M., and Watts, B. D. (1995). "Undrained shear strength for liquefaction flow failure analysis." *Can. Geotech. J.*, 32, 783–794.

Kramer, S. L., and Seed, H. B. (1988). "Initiation of soil liquefaction under static loading conditions." *J. Geotech. Eng.*, 114(4), 412–430.

Lade, P. V. (1992). "Static instability and liquefaction of loose fine sandy slopes." *J. Geotech. Eng.*, 118(1), 51–71.

Lade, P. V., and Duncan, J. M. (1973). "Cubical triaxial tests on cohesionless soil." *J. Soil Mech. Found. Div.*, 99(10), 793–812.

Lade, P. V., Nelson, R. B., and Ito, Y. M. (1987). "Nonassociated flow and stability of granular materials." *J. Eng. Mech.*, 113(9), 1302–1318.

Lade, P. V., Nelson, R. B., and Ito, Y. M. (1988). "Instability of granular materials with nonassociated flow." *J. Eng. Mech.*, 114(12), 2173–2191.

Lancelot, L., Shahrour, I., and Al Mahmoud, M. (2003) Experimental study of sand behavior at low stresses in Deformation Characteristics of Geomaterials, H. Di Benedetto et al., eds., Swets & Zeitlinger, Lisse, The Netherlands, 655–662.

Lee, K. L. (1978) "End restraint effect on undrained static triaxial strength of sand." *J. Geotech. Eng. Div., Am. Soc. Civ. Eng.*, 104, 687–704.

Menzies, B. (1988) "A computer controlled hydraulic triaxial testing system." *Advance triaxial testing of soil and rock, ASTM STP 977*, R. T. Donaghe, R. C. Chaney, and M. L. Silver, eds., ASTM, Philadelphia, 82–94.

Saada, A., and Bianchini, G. (1988). *Constitutive equations for granular noncohesive soils*, Balkema, Rotterdam, The Netherlands.

Sladen, J. A., D'Hollander, R. D., and Krahn, J. (1985). "The liquefaction of sands, a collapse surface approach." *Can. Geotech. J.*, 22, 564–578.

Tatsuoka, F., Sakamoto, M., and Kawamura, T. (1986). "Strength and deformation characteristics of sand in plane strain compression at extremely low pressures." *Soils Found.*, 26(1), 65–84.